AMERICAN SOCIETY FOR MICROBIOLOGY | Microbiology Spectrum

| Virology | Research Article

Swine influenza A virus isolates containing the pandemic H1N1 origin matrix gene elicit greater disease in the murine model

Shelly J. Curran,[1,2,3] Emily F. Griffin,[1,2,3] Lucas M. Ferreri,[4] Constantinos S. Kyriakis,[2,3] Elizabeth W. Howerth,[5] Daniel R. Perez,[4] S. Mark Tompkins[1,2,3]

AUTHOR AFFILIATIONS See affiliation list on p. 14.

ABSTRACT Since the 1990s, endemic North American swine influenza A viruses (swFLUAVs) contained an internal gene segment constellation, the triple reassortment internal gene (TRIG) cassette. In 2009, the H1N1 pandemic (pdmH1N1) virus spilled back into swine but did not become endemic. However, the pdmH1N1 contributed the matrix gene (pdmM) to the swFLUAVs circulating in the pig population, which replaced the classical swine matrix gene (swM) found in the TRIG cassette, suggesting the pdmM has a fitness benefit. Others have shown that swFLUAVs containing the pdmM have greater transmission efficiency compared to viruses containing the swM gene segment. We hypothesized that the matrix (M) gene could also affect disease and utilized two infection models, resistant BALB/c and susceptible DBA/2 mice, to assess pathogenicity. We infected BALB/c and DBA/2 mice with H1 and H3 swFLUAVs containing the swM or pdmM and measured lung virus titers, morbidity, mortality, and lung histopathology. H1 influenza strains containing the pdmM gene caused greater morbidity and mortality in resistant and susceptible murine strains, while H3 swFLUAVs caused no clinical disease. However, both H1 and H3 swFLUAVs containing the pdmM replicated to higher viral titers in the lungs and pdmM containing H1 viruses induced greater histological changes compared to swM H1 viruses. While the surface glycoproteins and other gene segments may contribute to swFLUAV pathogenicity in mice, these data suggest that the origin of the matrix gene also contributes to pathogenicity of swFLUAV in mice, although we must be cautious in translating these conclusions to their natural host, swine.

IMPORTANCE The 2009 pandemic H1N1 virus rapidly spilled back into North American swine, reassorting with the already genetically diverse swFLUAVs. Notably, the M gene segment quickly replaced the classical M gene segment, suggesting a fitness benefit. Here, using two murine models of infection, we demonstrate that swFLUAV isolates containing the pandemic H1N1 origin M gene caused increased disease compared to isolates containing the classical swine M gene. These results suggest that, in addition to other influenza virus gene segments, the swFLUAV M gene segment contributes to pathogenesis in mammals.

KEYWORDS influenza virus, pathogenesis, swine influenza, mouse model, matrix gene, pandemic influenza

Influenza is considered a major public health threat causing between 250,000 and 300,000 deaths annually worldwide (1–3). Influenza A viruses (FLUAVs) are single-stranded, negative-sense RNA viruses with a segmented genome containing eight gene segments (4). These include the hemagglutinin (HA) and neuraminidase (NA) genes, which encode the surface glycoproteins forming the spikes on the outside of the virion and determine the virus subtype, the internal protein genes which include three polymeraseS, polymerase basic 1 (PB1), polymerase basic 2 (PB2), and polymerase acidic

Editor Robert Paul de Vries, Universiteit Utrecht, the Netherlands

Address correspondence to S. Mark Tompkins, smt@uga.edu.

Shelly J. Curran and Emily F. Griffin contributed equally to this article. Author order was determined on the basis of initiating and completing the research and manuscript.

The authors declare no conflict of interest.

See the funding table on p. 15.

Received 22 September 2023
Accepted 8 January 2024
Published 1 February 2024

(PA) genes, as well as the nucleoprotein (NP), non-structural (NS) and the matrix (M) segments (4).

The M gene encodes two proteins, M1 and M2. M2 is a 97-amino acid (aa), well-characterized proton channel which contributes to the release of viral RNA from the virion during infection (5) as well as virus budding (6). The M2 proton channel also interacts with the host immune response modifying inflammasome activation (7) and autophagy (8–10). The 252-aa M1 protein bridges the viral ribonucleoprotein complexes (RNPs) and membrane proteins. It plays an important role in the release of viral RNA from the virion during infection, export of the viral RNPs out of the nucleus, inhibition of reimport of RNPs, and assembly of virus particles. The M1 protein is a determinant of the characteristic pleomorphic morphology of influenza virus particles, with filamentous virus particles linked to increased neuraminidase activity, affecting transmission (11–13).

Similar to humans, FLUAVs have been enzootic in swine worldwide, causing respiratory disease outbreaks in herds characterized by high morbidity, low mortality, and significant economic losses (14). For almost eight decades, a single H1N1 FLUAV, known as "classical" swine influenza, was circulating in the North American swine population (15, 16). However, in the late 1990s, novel triple reassortant H1N1, H1N2, and H3N2 viruses emerged in pigs containing gene segments from classical swine, human, and avian origin FLUAVs (17, 18). The six internal gene segments, known as the triple reassortment internal gene (TRIG) cassette, became predominant, such that since 2000, most fully characterized North American swine influenza strains contain this internal protein gene combination with varying HA and NA combinations (16, 17, 19–22). Since the pandemic of 2009, which was caused by a novel reassortant swine-origin H1N1 virus with gene segments from North American swine viruses and an avian-like H1N1 Eurasian swine virus (23), the necessity for surveillance of the spread and genetic diversity of swine influenza viruses has become evident. Recent studies have shown regional differences in circulating strains both in the United States as well as in other countries, with a diversification of genetic constellations and multiple HA and NA subtypes and clades in cocirculation (24–32). At the same time, field surveillance has demonstrated that since 2011, the pandemic origin M gene segment (pdmM) has been systematically replacing the swine TRIG M gene segment (swM) in North American swine FLUAVs, with up to 70% of swine influenza A virus (swFLUAVs) containing the pdmM gene in 2011 and increasing to 100% by 2015 (30, 33–35). The pdmM gene is commonly found in swFLUAVs isolated at state fairs (36), and the M gene segment has been shown to be under differential selective pressure based upon different hosts, possibly influencing host tropism and immune response (37, 38). The pdmM gene has also been linked to increased neuraminidase activity and increased transmissibility when combined with NA from the laboratory virus A/PR/8/1934 H1N1 or the original pandemic virus A/NL/602/2009 (13) or the NA from a Eurasian H1N1 virus (39). However, the influence of the pdmM gene on disease in the context of native swine HA and NA gene segments in wild-type viruses has not been explored.

The murine model is one of the most common animal models used for FLUAV pathogenesis research. Previous studies have shown a variation in pathogenesis between inbred strains of mice, demonstrating a contribution of genetic background to influenza-elicited disease and resulting in categorization of a continuum from susceptible to resistant (40). Susceptible strains, such as DBA/2, demonstrate higher morbidity, mortality, and viral replication, while their immune response is characterized by greater concentrations of proinflammatory cytokines and increased numbers of lung infiltrates in response to influenza infection compared to resistant mouse strains such as BALB/c. These two mouse models have been used to assess disease severity with a variety of influenza viruses, including H1, H3, H5, and H7 viruses (40, 41). The susceptibility of DBA/2 mice to infection and severe disease has resulted in use of this mouse model for antiviral drug and vaccine efficacy studies (42, 43).

We hypothesized that infection of mice with swine FLUAV strains containing the pdmM gene would result in greater morbidity and mortality and induce more severe

lung lesions compared to infection with strains of the same subtype and combination of gene segments containing the swM gene. We used both DBA/2 and BALB/c mice to define the infection and disease phenotypes of swine influenza isolates to differentiate the contribution of the M gene in susceptible and resistant murine strains. We define virus replication kinetics, clinical disease, and pathology elicited by swM and pdmM gene-containing viruses, demonstrating increased disease severity elicited by viruses with the pdmM gene.

RESULTS

The matrix gene contributes to morbidity and mortality of swine H1 influenza infection in mice

The TRIG cassette consists of the six internal gene segments, PB2, PB1, PA, NP, M, and NS (Fig. 1A, light blue). We assessed the influence of the M gene segment on pathogenicity by comparing disease elicited by swine FLUAV strains with related HA and NA gene segments and for the internal gene segments, differing primarily in the M gene (Fig. 1A, light blue versus red). To reflect the potential for different morbidity and mortality outcomes dependent on the host, we inoculated both resistant (BALB/c) and susceptible (DBA/2) mouse strains (44) with a panel of swine H1 FLUAVs spanning a variety of HA and NA clades and containing either the swM or pdmM gene segment (n = 5 mice/group) (Fig. 1A). The H1 viruses containing the pdmM caused greater morbidity, as demonstrated by weight loss, and mortality in both resistant BALB/c (Fig. 1B and C) and susceptible DBA/2 (Fig. 1D and E) mouse strains. As previously shown by others, infection of mice with H3 viruses of human or swine origin resulted in minimal morbidity or mortality without adaptation (41, 45). To investigate whether the pandemic origin matrix gene can induce greater morbidity or mortality in mice infected with swine H3 influenza strains, we inoculated both resistant BALB/c and susceptible DBA/2 murine strains with H3 influenza strains differing only in the matrix gene (n = 5 mice/group). Both resistant and susceptible mouse strains showed no morbidity, as determined by weight loss (Fig. 2), or mortality (data not shown) when infected with H3 strains containing either the pdmM or swM gene segments.

The matrix gene contributes to increased viral replication in the lungs of infected mice

Influenza-mediated morbidity and mortality in mouse models can be attributed to viral replication and immune mediated damage. In order to determine whether viral replication contributes to the greater morbidity and mortality caused by FLUAV strains containing the pdmM gene segment, we inoculated resistant and susceptible murine strains with swFLUAVs and assessed virus replication kinetics by lung virus titer (n = 5 mice/virus/collection time point). The H1 influenza viruses containing the pdmM gene segment replicated to significantly higher (between 1 and 4 logs greater) viral titers at 2 days post infection (DPI) and maintained significantly higher viral titers through 6 DPI in the resistant BALB/c mice (Fig. 3A). The same viruses replicated only slightly better, 2–3 logs greater lung viral titers, than the swM-containing virus in the susceptible DBA/2 mouse strain, apart from NC/702/pdmM, which replicated similarly to the MO/664/swM virus (Fig. 3B). Lung virus titers were also compared between H3 viruses containing pdmM or swM gene segments, in resistant and susceptible mouse strains. While neither of the swine H3 influenza viruses caused clinical signs, the viruses did replicate in mice, albeit at lower peak viral titers compared to the H1 swFLUAVs. Notably, NC/671/pdmM replicated to higher viral titers compared to MN/993/swM and was detectable through 6 DPI, while MN/993/swM was cleared after 4 DPI (Fig. 3C). In the susceptible DBA/2 mouse strain, no significant differences were observed in virus replication kinetics, although titers following pdmM-containing H3N2 viral infection were consistently slightly higher until cleared after 6 DPI (Fig. 3D). The robust replication of non-mouse-adapted H3N2 influenza viruses in mice was unexpected, so we assessed several human-origin H3N2

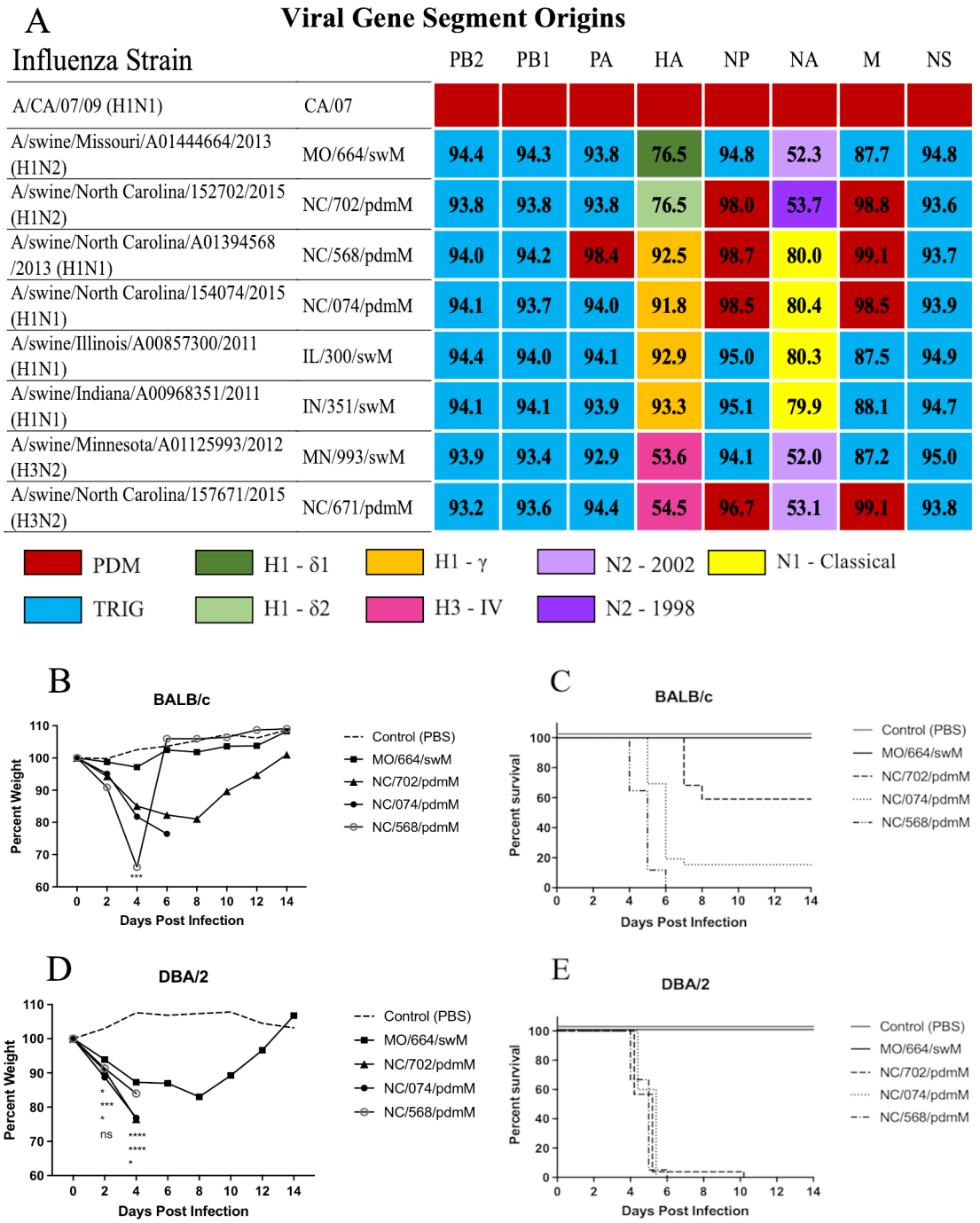

FIG 1 Influenza viruses used for mouse infections and morbidity and mortality in mice. (A) The origin of each gene segment is color coded according to the key. Numbers indicate percent nucleotide sequence homology compared to A/CA/04/2009 (pdmH1N1). (B and D) Percent weight loss and (C and E) mortality of (B and C) BALB/c or (D and E) DBA/2 mice following infection with indicated swine H1 influenza viruses. Mice were inoculated with 1e5 PFU of virus (*n* = 5 per group) and weights were recorded every other day. This study was repeated to confirm results. Statistical comparison between MO/664/swM and the other viruses by two-way analysis of variance with Dunnett post hoc test (B and D). *<0.05, ***<0.001, ****<0.0001. Kaplan-Meier survival curves (C and E). Abbreviations: HA, hemagglutinin; M, matrix; NA, neuraminidase; NP, nuclear protein; ns, not signficant; NS, non-structural; PA, polymerase acidic; PB1, polymerase basic 1; PB2, polymerase basic 2; PDM, pandemic 2009 lineage; pdmH1N1, H1N1 pandemic; TRIG, triple reassortment internal gene constellation.

(huH3) viruses for replication in BALB/c and DBA/2 mice. While the swine H3N2 viruses replicated in mice without causing disease, huH3 viruses having HA and NA genes segments related to the swFLUAVs failed to replicate in either mouse strain, with no detectable virus in the lung at 2 DPI (data not shown). The greater lung viral titers of both

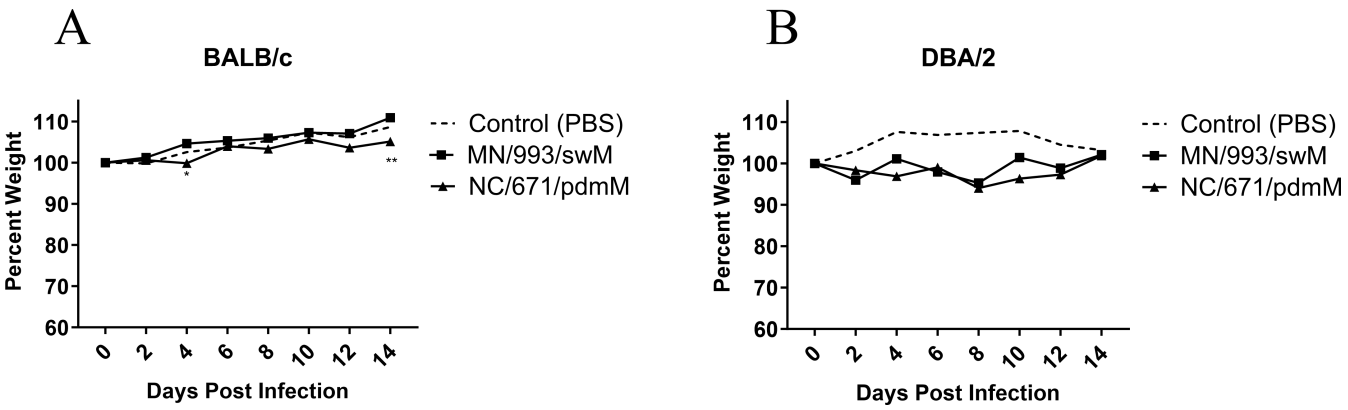

FIG 2 Morbidity of mice infected with swine H3 influenza viruses. (A) BALB/c or (B) DBA/2 mice were inoculated with 1e5 PFU of the indicated viruses (n = 5 mice/group, repeated), and weights were recorded every other day. Statistical comparison between MN/993/swM and NC/671/pdmM by two-way analysis of variance with Bonferroni post hoc test. **<0.005. PBS, phosphate-buffered saline.

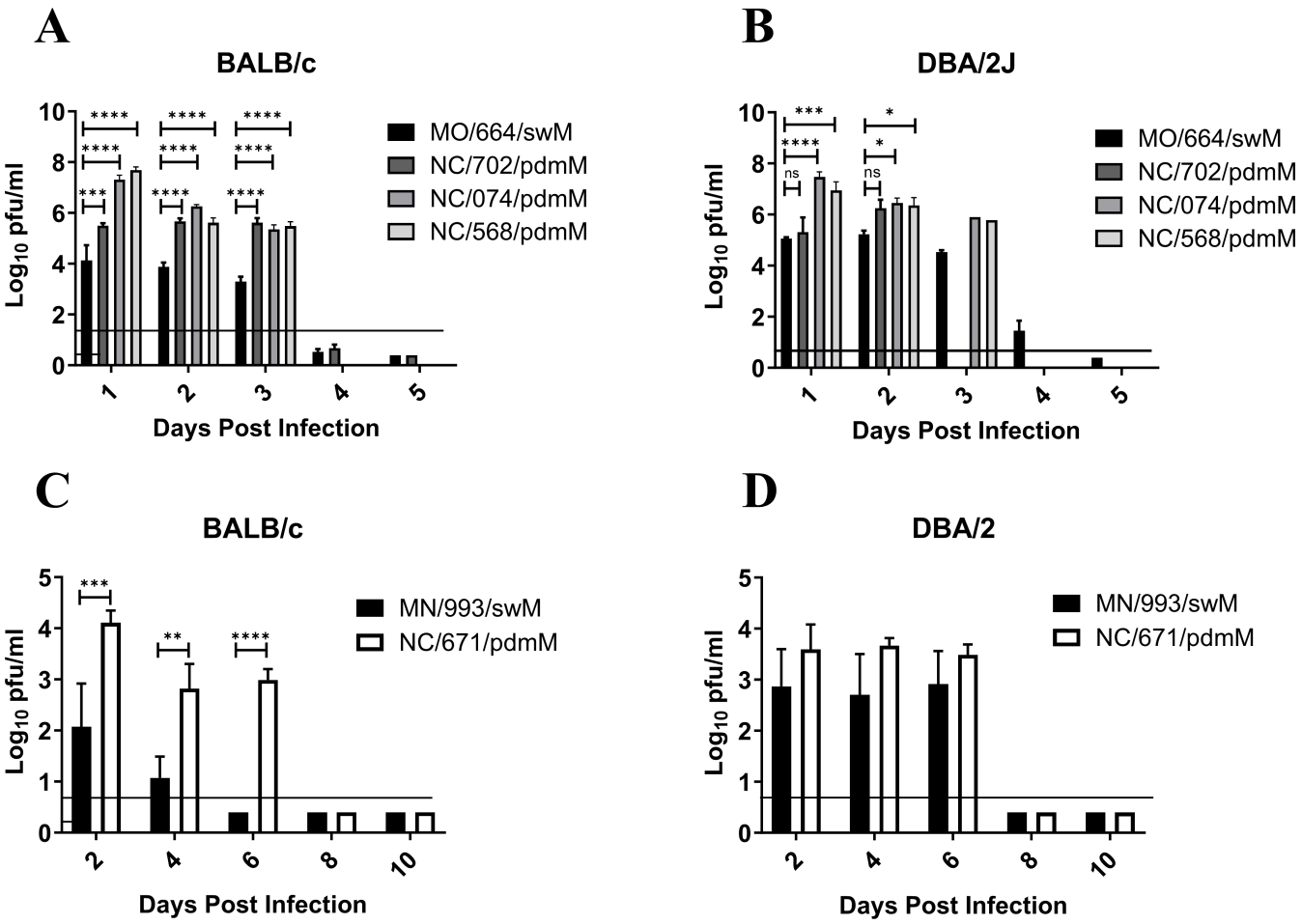

FIG 3 Lung virus titers over time from mice infected with swine H1 and H3 influenza viruses. (A and C) BALB/c and (B and D) DBA/2 mice were inoculated with 1e5 PFU of the indicated viruses. Lungs collected at indicated time points, homogenized, and assayed for virus titer by plaque assay (n = 5 mice/group/collection time point, repeated). Statistical comparison between (A and B) MO/664/swM and the other viruses was completed using two-way analysis of variance (ANOVA) with Dunnett post hoc test or (C and D) MN/993/swM and NC/671/pdmM by two-way ANOVA with Bonferroni post hoc test. *<0.05, **<0.005, ***0.001, ****<0.0001.

H1 and H3 influenza strains containing the pandemic origin matrix gene has the potential to induce greater pathology in the lungs; therefore, we next assessed the lungs of influenza-infected mice for histopathological changes.

The pandemic origin matrix gene contributes to greater disease and more severe histological changes in the lungs of influenza-infected mice

In order to understand the development of disease and evaluate the characteristics and extent of lesions induced in the lung, we inoculated both resistant (BALB/c) and susceptible (DBA/2) mice with the panel of swFLUAVs and assessed histopathological changes in the lung at 2 and 4 DPI (n = 2 mice/virus/collection time point). Mice inoculated with MO/664/swM had mild pulmonary changes on 2 DPI characterized by a small number of bronchioles with mild segmental necrosis of the epithelium and minimal peribronchiolar infiltrations of lymphocytes admixed with neutrophils. In addition, a small number of vessels with mild perivascular infiltrations of lymphocytes admixed with fewer neutrophils and rare foci of alveoli containing small numbers of neutrophils and macrophages were present (data not shown). Changes were slightly more severe on 4 DPI (Fig. 4A and E). The number of involved bronchioles and vessels increased but was still less than 25%, and there was an increased amount of epithelial necrosis and numbers of peribronchiolar and perivascular inflammatory cells. Susceptible DBA/2 mice were similarly infected with MO/664/swM, and lung analyses were conducted for pathological changes. Mild to moderate interstitial changes were present in the DBA/2 mice, characterized by mild multifocal alveolar infiltrations of a small number of neutrophils and macrophages (data not shown).

The resistant BALB/c mice inoculated with NC/702/pdmM, NC/074/pdmM, or NC/568/pdmM had similar pulmonary changes on 2 DPI compared to mice inoculated with MO/664/swM; however, histopathology was more severe, ranging from mild to moderate overall (Fig. 4E), with larger numbers of involved bronchioles and vessels, more extensive epithelial necrosis, and increased numbers of perivascular and peribronchiolar lymphocytes admixed with neutrophils (data not shown). Pulmonary changes increased from mild to moderate in the NC/702/pdmM mice by 4 DPI (Fig. 4B). However, in the NC/074/pdmM and NC/568/pdmM mice, changes were already moderate on 2 DPI, with the NC/568/pdmM inoculated mice being the most severe of all the groups. The resistant BALB/c mice inoculated with the pdmM-containing viruses had more extensive and severe interstitial involvement than seen in the swM-inoculated mice, which increased in extent and severity of involvement by 4 DPI, being most severe in mice inoculated with NC/568/pdmM (Fig. 4E). In NC/702/pdmM and NC/074/pdmM inoculated mice, interstitial involvement ranged from mild (< 25%) on 2 DPI to moderate (25%–50%) by 4 DPI and was characterized by foci with slightly thickened alveolar septa and small numbers of neutrophils, lymphocytes, and macrophages in alveoli to foci, where alveoli were filled with large numbers of inflammatory cells and necrotic debris (Fig. 4B and C). In NC/568/pdmM inoculated mice, interstitial involvement was already moderate on 2 DPI (data not shown) with >50% involvement of the parenchyma by 4 DPI (Fig. 4D). Interstitial foci were similar to mice inoculated with NC/702/pdmM and NC/074/pdmM but also included foci with moderately thickened alveolar septa with mild epithelial hyperplasia. Mice inoculated with NC/568/pdmM by 4 DPI had multifocal interstitial hemorrhage that was more severe than with any of the other virus isolates (Fig. 4D) and included the development of hyaline membranes in DBA/2 mice, which suggests more extensive alveolar septal damage with the NC/568/2013 isolate. Overall, there were significantly greater pulmonary changes in mice inoculated with swFLUAVs containing the pdmM gene segment compared to the virus containing the swM gene segment (Fig. 4E). Similar results were observed in swFLUAV-infected, susceptible DBA/2 mice, although the differences lacked statistical significance (Fig. S1A).

Resistant BALB/c and susceptible DBA/2 mice were also inoculated with H3 swFLUAVs containing either the pdmM or swM gene, and histopathological changes were assessed in the lung at 2 and 4 DPI (n = 2 mice/virus/collection time point). On 2 DPI, lungs from

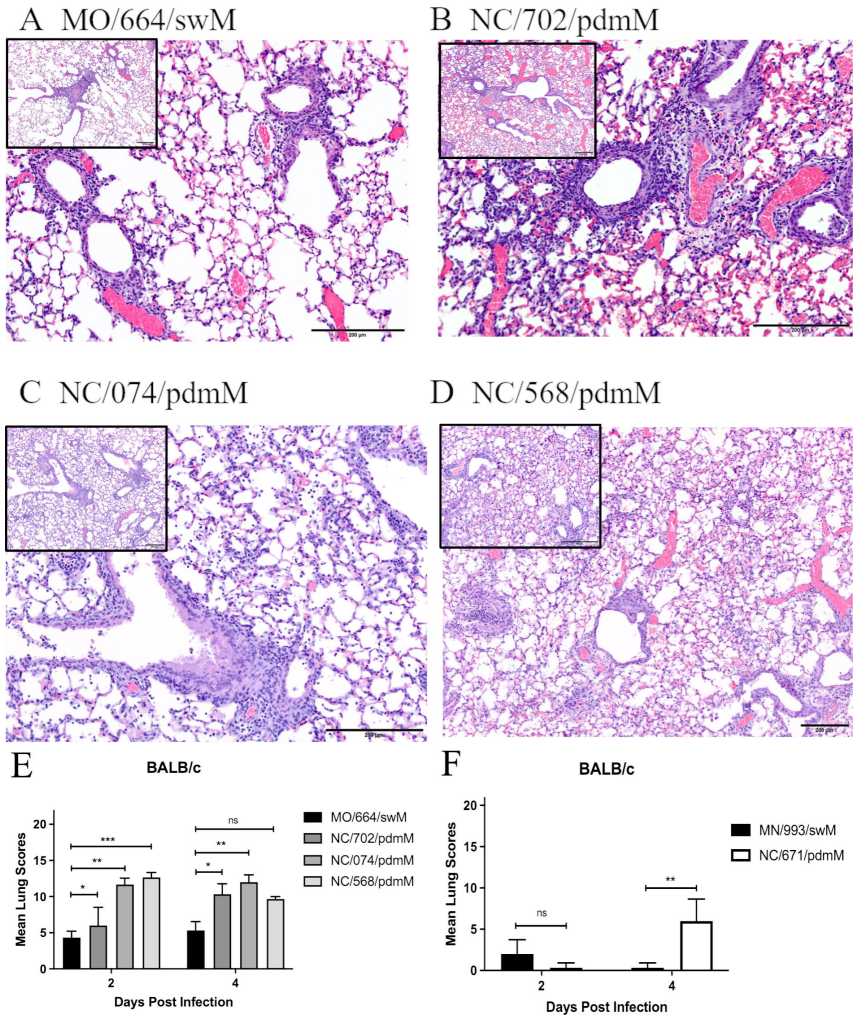

FIG 4 Histological images and lesion scores from mice infected with swine influenza viruses. BALB/c mice were inoculated with 1e5 PFU of the indicated viruses and euthanized, and the lungs were fixed for histological analysis at 2 and 4 DPI (n = 2 mice/virus/collection, repeated). Lungs were assigned histological lesion scores out of 22. (A–D) Images of lung sections from 4 DPI at 20× and 10× (inset) for A/swine/Missouri/A01444664/2013 (H1N2) (A), A/swine/North Carolina/152702/2015 (H1N2) (B), A/swine/North Carolina/154074/2015 (H1N1) (C), and A/swine/North Carolina/A01394568/2013 (H1N1) (D). (A) MO/664/swM: mild perivascular and peribronchiolar infiltrations of mostly lymphocytes and mild segmental necrosis of the bronchiolar epithelium are present, but there are no significant interstitial changes. Lesion score: 6 out of 22. (B) NC/702/pdmM: bronchioles are dilated and there are moderate peribronchiolar and mild perivascular infiltrations of mostly lymphocytes and diffuse necrosis of the bronchiolar epithelium. Focally extending from the central bronchiole, alveolar septa are thickened and there are small numbers of inflammatory cells in the alveoli. Lesion score: 10 out of 22. (C) NC/074/pdmM: bronchioles are slightly dilated with mild epithelial necrosis and sloughed epithelial cells and a few inflammatory cells in the lumen. There are mild to moderate peribronchiolar and perivascular infiltrations of mostly lymphocytes. Diffusely, the alveolar septa are mildly thickened, and the alveoli contain small numbers of inflammatory cells. Lesion score: 13 out of 22. (D) NC/568/pdmM: bronchioles are slightly dilated and lined by the attenuated epithelium. There are mild peribronchiolar and perivascular infiltrations of mostly lymphocytes. Diffusely, the alveolar septa are mildly thickened, and alveoli contain small numbers of inflammatory cells admixed with erythrocytes. Lesion score: 10 out of 22. (E and F) Histological lesion scores out of 22 for BALB/c mice inoculated with either the H1 or H3 swine influenza isolates. Statistical differences were calculated using two-way ANOVA between (E) MO/664/swM and the other viruses with Dunnett post hoc test or (F) MN/993/swM and NC/671/pdmM with Bonferroni post hoc test. *<0.05, **<0.005, ***<0.001.

BALB/c mice inoculated with MN/993/swM or NC/671/pdmM had minimal changes that were not specific for influenza, however by 4 DPI, mice inoculated with NC/671/pdmM had mild pulmonary changes consistent with influenza infection in contrast to minimal non-specific changes in MN/993/swM infected mice (Fig. 4F). Pathological changes were overall similar in DBA/2 and BALB/c mice; however, pathology was slightly more severe in BALB/c mice and included minimal to mild lymphocytic infiltrations around a small number of bronchioles and vessels and minimal to mild segmental epithelial necrosis in a few larger apical bronchioles (Fig. S1B). Together these data suggest that the pandemic origin matrix gene induces greater pathological changes in the lung resulting in greater severity of disease in both susceptible DBA/2 and resistant BALB/c murine strains. However, differences in H1 and H3 swFLUAVs suggest the HA and NA, as well as the overall gene composition can influence the pathogenicity of a particular influenza strain. To further address this possibility, we infected both resistant BALB/c and susceptible

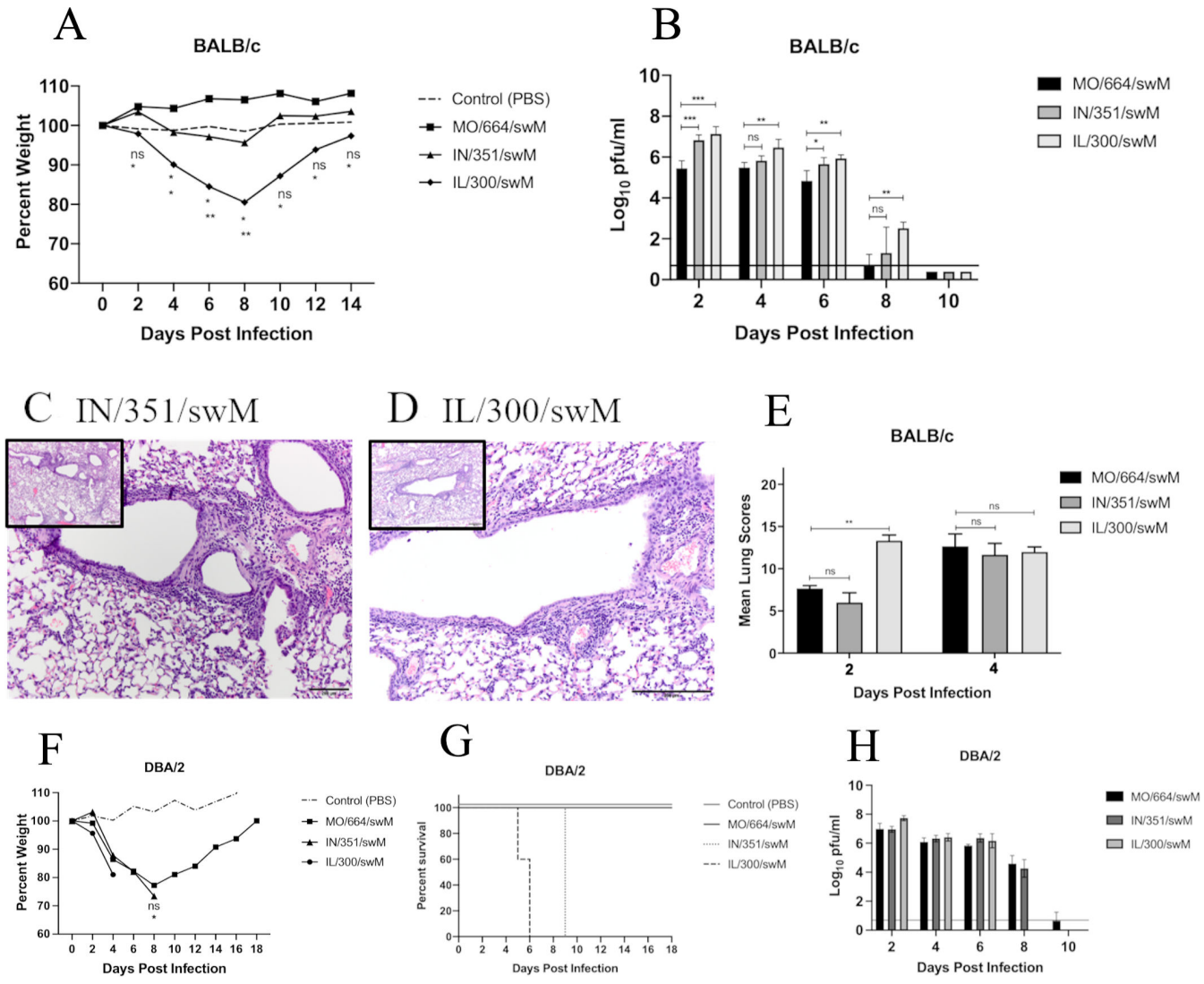

FIG 5 Morbidity, mortality, histology, and lung virus titers of mice infected with alternate swine H1 influenza viruses. (A–E) BALB/c mice were inoculated with 1e5 PFU of the indicated viruses and (A) weights were recorded every other day and lungs collected and (B) assayed for virus titer or (C–E) histopathology ($n = 5$ mice/virus/collection for titers, $n = 2$ mice/virus/collection for histopathology, repeated). Images of lung sections from (C) A/sw/Indiana/A00968351/2011 (H1N1, IN/351/swM) or (D) A/sw/Illinois/A00857300/2011 (H1N1, IL/300/swM) infected mice, 4 DPI at 20× and 10× (inset) and (E) histological lesion scores out of 22. DBA/2 mice were inoculated with 1e5 PFU of the indicated viruses and (F) weights and (G) survival were recorded, or (H) lungs were collected and assayed for virus titer. Statistical differences were calculated between MO/664/swM and the other viruses by two-way ANOVA with Dunnett post hoc test. *<0.05, **<0.005, ***<0.001, ****<0.0001.

DBA/2 strains with a panel of H1 influenza strains containing the swM gene but varying either in their HA or NA segments.

The HA and NA gene segments can impact disease severity of swM gene-containing viruses

To determine whether swine H1 influenza strains containing the swM gene with either HA or NA gene segments of different lineages or subtypes can cause greater morbidity, mortality, and severity of disease, we inoculated both resistant BALB/c and susceptible DBA/2 mouse strains with an alternate panel of FLUAVs with HA and NA gene compositions differing from the MO/664/swM strain (H1 delta 1 cluster and N2 subtype, n = 5 mice/virus/collection time point). The swFLUAVs IN/351/swM and IL/300/swM contain HA gene segments from the gamma cluster and NA gene segments from the classical N1, which are comparable to the HA and NA segments of NC/568/pdmM and NC/074/pdmM viruses (Fig. 1A). Nucleotide and predicted amino acid sequence comparisons were analyzed to ensure high homology among PB2, PB1, PA, NP, and NS genes (≥91% nucleotide and ≥92% predicted amino acid homology) as well as within HA and NA clusters (Fig. 1A; Table S2). In the resistant BALB/c mouse strain, the alternate H1 FLUAV strains containing the swM gene induced greater morbidity, as determined by weight loss, but not greater mortality (Fig. 5A), despite replicating to significantly higher titers in the lung (Fig. 5B). In the susceptible DBA/2 strain, the alternate H1 swM-containing strains did cause both greater morbidity and mortality without replicating to significantly higher titers (Fig. 5F through H) unlike the pdmM containing viruses seen previously. Due to the potential for the increased replication of IN/351/swM and IL/300/swM to induce greater pathology, we evaluated the lungs for histopathological changes (n = 2 mice/virus/collection time point).

For both murine models, on day 2, the predominant lesion was in the bronchioles characterized by epithelial necrosis and minimal interstitial changes consistent among the three swFLUAVS MO/664/swM, IN/351/swM, and IL/300/swM (data not shown). By day 4, in both the resistant BALB/c (Fig. 5C and D) and susceptible DBA/2 strains (data not shown), there were no significant differences in lung pathology scores for the three swM gene-containing viruses (Fig. 5E). Vasculitis was present with all three swFLUAVs in BALB/c and DBA/2 mice (data not shown). While the results comparing pdmM and swM gene-containing viruses suggested the swM virus elicited limited pulmonary differences compared to the pdmM gene-containing viruses (Fig. 4), comparison with the viruses containing alternate HA or NA genes and the swM gene showed variable pulmonary differences in the lungs of infected mice (Fig. 5E), suggesting the HA or NA may be contributing to pathogenesis in the absence of differences in the origin of the M gene segment.

DISCUSSION

Multiple introductions of the 2009 pH1N1 virus into the swine population have led to reassortment events with previously circulating swine FLUAVs, resulting in hitherto unseen genetic constellations. Prior research has shown the matrix gene from the pandemic virus is replacing the classical swine origin matrix gene found in the TRIG cassette, suggesting an evolutionary advantage or fitness benefit. We used resistant BALB/c and susceptible DBA/2 mouse strains to investigate whether infection with swine influenza isolates containing the pandemic origin matrix gene (pdmM) would induce greater disease compared to isolates containing the classical swine origin matrix (swM) gene. We chose influenza isolates reflecting the predominant strains found in North America between 2010 and 2016 (33). Infection with H1 influenza viruses containing the pdmM resulted in greater morbidity and mortality in both susceptible DBA/2 and resistant BALB/c mouse strains. However, infection with H3 isolates containing either the pdmM or swM did not induce morbidity or mortality, which is in agreement with

previous studies that have shown a very high lethal dose for earlier swine H3 viruses and an inability to infect mice with human H3N2 strains (41).

We evaluated virus replication in the lungs of both susceptible (DBA/2) and resistant (BALB/c) mice. Both H1 and H3 swFLUAVs containing the pdmM replicated to higher viral titers in the lungs of susceptible DBA/2 and resistant BALB/c mice compared to swFLUAVs containing the swM. Higher viral titers in the mouse lungs suggests that the pdmM gene confers increased infectivity or replication efficiency within the mice at least to some degree. The higher viral load in the lungs may contribute to the greater morbidity and mortality observed in pdmM-containing influenza virus-infected mice. However, in comparing several swM-containing viruses, we observed varying lung virus titers in BALB/c mice without concomitant differences in mortality, and in contrast, no differences in lung virus titer yet clear differences in survival in susceptible DBA/2 mice. Thus, while the M gene may affect outcomes of infection, other gene segments also impact infection and disease and are additionally influenced by the host genetic background. These differences could be due to virus replication at the cellular level or the host immune response to infection.

Others have compared outcomes of influenza virus infection in susceptible versus resistant mouse strains with avian H5N1 (46), mouse-adapted H1N1 (A/PR/8/1934) (47) or H3N2 (A/HKX-31) (48), or mouse-adapted classical swine H1N1 (49) virus. Influenza viruses replicated to higher titers in susceptible DBA/2 mice compared to resistant (BALB/c or C57Bl/6) mice in all of these studies and were correlated with increased inflammatory responses as well as increased disease severity and mortality. In contrast, virus titers were not entirely correlated with morbidity and mortality in DBA/2 and BALB/c mice when infected with swFLUAVs containing swM or pdmM genes. The H1 influenza viruses containing the pdmM gene replicated to similarly high titers in BALB/c and DBA/2 mice, resulting in greater morbidity and mortality compared to the swM gene-containing H1 virus, MO/664/swM, that replicated to lower virus titers and showed no mortality in either mouse strain. However, two other swM gene-containing H1 viruses replicated to higher titers in BALB/c mice but did not cause mortality. Furthermore, the three swM H1 viruses, MO/664/swM, IN/351/swM, and IL/300/swM, replicated to similar titers in DBA/2 mice with variable mortality. Finally, the tested H3N2 swFLUAVs replicated to similar or slightly lower titers compared to the H1N2 MO/664/swM virus, with the swM gene-containing H3N2 virus replicating more poorly than the pdmM virus, but neither caused morbidity or mortality in BALB/c or DBA/2 mice. While total virus replication or peak viral load may contribute to disease severity between susceptible DBA/2 and resistant BALB/c mouse strains, other factors may be affecting disease severity.

Differences in the proinflammatory response between susceptible and resistant mouse strains have also been implicated in disease severity and mortality, with increases in proinflammatory cytokines and other inflammatory mediators observed in susceptible DBA/2 mice associated with increased disease severity and mortality following influenza virus infection. We did not assess cytokine responses here; however, histopathological changes were generally greater in DBA/2 mice compared to BALB/c mice, suggesting increased inflammation.

The influenza matrix gene has been shown to influence the inflammasome and autophagy (7–10) as well as to affect morphology, host range, and transmission (13, 37, 50). In humans, inflammation and development of pneumonia have been correlated with swine origin and pandemic H1N1 infection (51), while other studies have related an altered immune response with FLUAVs containing the pdmM gene (52). We assessed the development of microscopic changes in the lungs of swFLUAV-infected BALB/c and DBA/2 mice. Both H1 and H3 swFLUAVs containing the pdmM gene induced greater histological changes characterized by necrosis, increased infiltrates, thickening of the alveoli septa, and epithelial hyperplasia compared to viruses containing the swM gene. This was seen in both resistant BALB/c and susceptible DBA/2 mouse strains. The increased severity of lesions in the lungs of mice infected with an H3 swFLUAV containing the pdmM gene compared to the H3 virus containing the swM, while not as severe as

was seen with the H1 isolates, was evident despite a lack of significant difference in viral replication in the susceptible DBA/2 murine strain. Together, these data suggest that while greater viral replication by the swFLUAVs containing the pdmM gene contributes in part to the increased histopathological lesions in the lungs, other viral and host factors may also contribute to the enhanced lung lesions and subsequent disease. The lack of significant pulmonary changes in the lungs of mice infected with the panel of swFLUAVs containing the swM gene despite differences in replication supports this concept. Of note, the microscopic changes in the lung switched from bronchiolar to more interstitial over time in the mice inoculated with the H1 viruses containing the pdmM gene. In humans, interstitial damage, along with the development of hyaline membranes, has been associated with the development of severe influenza viral pneumonia (53). Furthermore, in mice as well as in humans, severe influenza viral pneumonia has been correlated with the dysregulation of inflammation of the airways (54–57). This suggests that the differential lung pathology may in part be due to the subsequent immune response to the infection and the potential for infection with swine influenza isolates containing the pandemic matrix gene to generate an exacerbated immune response in the murine model.

Studies using reverse genetic viruses would be useful in ascertaining to what degree the pandemic matrix gene influences virus replication, disease progression, and outcome in murine models. Others have shown the origin of viral segments such as PB1 and NS1 genes may also contribute to swine influenza strain virulence and disease (58, 59). Recently, a reverse genetic approach was used to compare influenza virus replication and disease in BALB/c mice, comparing a Eurasian-origin M gene with the pdmM gene in an Asian-origin H1N1 virus background (60). The pdmM gene conferred increased virus titers, mortality, and disease, supporting our hypothesis and observations, although the Eurasian M gene is distinct from the classical swM gene we assessed here (16). The M gene has been shown in reverse genetic studies to modulate NA activity in recombinant viruses containing N1 genes from the 2009 pandemic virus A/NL/602/2009, a historical laboratory isolate, A/Puerto Rico/8/1934 (13), or a Eurasian lineage N1 (39), with the last compared to a classical swine N1. The increased NA activity was associated with increased transmission. We assessed the pathogenicity of a panel of wild-type viruses containing swM or pdmM gene segments with N2 or classical swine N1 gene segments with approximately 40% or 80% homology with the NA genes tested. It is unclear whether the swine viruses containing the pdmM gene have increased NA activity or transmissibility or if the impact of the M gene on these phenotypes is limited to distinct NA clades or subtypes. Assessment of the role of the M gene in our model as well as transmission models by reverse genetics will be important.

The NP gene has been shown to play an important role in viral RNA expression and viral morphology, but less in known regarding pathogenicity (61–65). Analysis of several Eurasian swine H1N1 viruses identified three mutations in the NP protein that did influence pathogenicity in mice. Nucleoprotein mutations V313F and K305R resulted in increased pathogenicity at high doses; the individual mutations did not confer increased disease. In contrast, NP K357Q reduced disease severity (66). All of the viruses we tested had NP K305 and K357, while all of the swM-containing viruses had F313 and the pdmM containing viruses had V313 (data not shown). Based upon the work by Zhu and colleagues, we would not predict the K305, F313, and K357 in NP to increase disease compared to K305, V313, and K357 at lower challenge doses, and we observed the viruses with the F313 caused less severe disease overall. Nevertheless, based upon the virulence phenotype observed with Eurasian swine influenza viruses, reverse genetic experiments involving the matrix gene alone as well as matrix gene and NP recombinants together may confirm whether the origin of the NP gene contributes to the pdmM linked results found in these studies.

Others have assessed immune responses in susceptible and resistant mouse strains infected with avian, human (mouse-adapted human), and swine origin FLUAVs, noting increased proinflammatory immune responses in susceptible mouse strains (46–49).

Understanding differences in the immune response elicited by swM- compared to pdmM-containing swFLUAVs would further clarify mechanisms of increased disease in the different mouse strains and in the context of the matrix gene. The use of susceptible DBA/2 and resistant BALB/c mouse models allows for the further exploration of host factor influence in observed swM versus pdmM induced pathogenesis. The increased susceptibility of DBA/2 mice provides increases in sensitivity for differences in pathogenicity for apparently avirulent viruses tested in BALB/c mice. Further use of these models may help discern subtle differences in phenotype when exploring matrix gene interactions in a reverse genetics system to help define determinants contributing to both mild and severe influenza infection outcomes. These studies, along with the work reported here, will help define the impact of individual genes on virus replication, the host response to infection, and determinants of disease.

MATERIALS AND METHODS

Cell culture and virus propagation

Influenza viruses A/swine/Missouri/A01444644/2013 (H1N2, MO/664/swM), A/swine/North Carolina/A01394568/2013 (H1N1, NC/568/pdmM), A/swine/Minnesota/A01125993/2012 (H3N2, MN/993/swM), A/swine/Illinois/A00857300/2011 (H1N1, IL/300/swM), and A/swine/Indiana/A00968351/2001 (H1N1, IN/351/swM) were obtained from the United States Department of Agriculture National Veterinary Services Laboratories reagent resource (30). Influenza viruses A/swine/North Carolina/152702/2015 (H1N2, NC/702/pdmM), A/swine/North Carolina/154074/2015 (H1N1, NC/074/pdmM), and A/swine/North Carolina/157671/2015 (H3N2, NC/671/pdmM) were obtained through the swine influenza surveillance project of the NIAID Emory-UGA Center of Excellent in Influenza Research and Surveillance (28, 67). Viruses were propagated in Madin-Darby canine kidney (MDCK) cells (IRR FR-926) in Minimal Essential Medium [MEM (GIBCO)] with 0.002-µg tosyl phenylalanyl chloromethyl ketone trypsin (Worthington). Viruses were cultured to achieve stock titers above 1e6 PFU/mL. Influenza virus titers were assessed by plaque assay on MDCK cells as previously described (68). Briefly, a 24-well plate of MDCK cells was incubated with serial dilutions of virus at 37°C and 5% CO_2 for 1–2 hours. The supernatant was removed; 1 mL of 1:1 2.4% Avicel solution and overlay [MEM (GIBCO) with 1-M HEPES (GIBCO), 200-mM GlutaMAX-I, 7.5% $NaHCO_3$ (GIBCO), and antibiotic/antimycotic (GIBCO)] was added; and the cells were incubated at 37°C and 5% CO_2 for 48–72 hours prior to fixation with 80/20 methanol/acetone and staining with crystal violet.

Sequencing and analysis

For the sequencing of viral gene segments, viral RNA was isolated using RNAzolRT (Sigma-Aldrich) as per manufacturer's protocol. cDNA synthesis and PCR were performed using SuperScript III One-step RT-PCR (Invitrogen) as per manufacturer's protocol. Primers used were as follows: all eight genes, simultaneously, MBTUni-12 (forward) 5′-ACGCGTGATCAGCRAAAGCAGG-3′, MBTUni-13 (reverse) 5′-ACGCGTGATCAGTAGAAACAAGG-3′, PB2 (forward) 5′-AGCRAAAGCAGGTCAATTATATTCA-3′, PB2 (reverse) 5′-AGTAGAAACAAGGTCGTTTTTAAACTA-3′, PB1 (forward) 5′-AGCRAAAGCAGGCAAACCATTTGAATG-3′, PB1 (reverse) 5′-AGTAGAAACAAGGCATTTTTTCATGAA-3′, PA (forward) 5′-AGCRAAAGCAGGTACTGATYCGAAATG-3′, and PA (reverse) 5′-AGTAGAAACAAGGTACTTTTTTGGACA-3′. NGS was performed using the Illumina MiSeq platform. All sequences are publicly available in GenBank. Virus isolates sequenced for this study are listed under NCBI bioproject accession number PRJNA600894 (Table S1). Sequences were aligned using MUSCLE alignment and comparison of predicted amino acids using Geneious (Biomatters Ltd.). Sequences of each of the genes of the isolates were compared to reference genes of pandemic origin, TRIG origin, and classical swine origin. Genes were categorized by the highest percentage similarity between the isolate gene and the reference sequence (Table S2).

Illumina MiSeq sequencing platform

Amplicon purification and library preparation

The PCR products were purified using Agencourt AMPure XP Magnetic Beads (Beckman Coulter) at 0.45× and eluted in 30 µL of HyClone molecular biology water (Genesee Scientific). The concentrations of the eluates were measured using the Qubit dsDNA HS Assay kit (ThermoFisher) on the Qubit v.3.0 fluorometer (ThermoFisher). Normalization was done at 0.2 ng/µL. Adapters were added using the Nextera XT DNA library preparation kit (Illumina) with 40% of the suggested final volume. The libraries were cleaned using 0.7× Agencourt AMPure XP Magnetic Beads, and the fragment size distribution was evaluated on the Agilent Bioanalyzer using the High Sensitivity DNA kit (Agilent). Thereafter, the samples were normalized to 4 nM. The pooled libraries were loaded at a concentration of 15 pM and sequenced using the MiSeq v.2, 300 cycle reagent Kit (Illumina) in a paired - end fashion (150 × 2).

Genome assembly

Genome assembly was performed using a pipeline developed previously by Harm Van Bakel from Icahn School of Medicine at Mount Sinai (69). Initially, Cutadapt was used to remove low-quality sequences and adapters from paired fastq files. The initial assembly was conducted using the inchworm module of Trinity (70). Viral contigs containing internal deletions were detected by mapping against non-redundant IRD reference sequencing using BLAT (71). Afterward, the inchworm assembly was iterated to eliminate breakpoint-spanning kmers. The resulting contigs were then oriented and trimmed, removing low-coverage ends as well as extraneous sequences beyond the conserved FLUAV termini. Finally, to evaluate assembly contigs and contiguity for all segments, sequences reads were mapped back to the ultimate assembly using Burrows - Wheeler alignment (72).

Mice

Female 6- to 8-week-old BALB/c mice were purchased from Charles River Laboratories (Raleigh, NC). Female 6- to 8-week-old DBA/2 mice were purchased from Jackson Laboratories (Bar Harbor, ME). All animal studies were approved by the Animal Care and Use Committee of the University of Georgia and carried out in strict accordance with the National Institutes of Health Guide for the Care and Use of Laboratory Animals. Humane euthanasia of mice followed American Veterinary Medical Association guidelines. All murine experiments were repeated to confirm findings and increase robustness.

In vivo infection

Mice were anesthetized by isoflurane (Patterson Veterinary) inhalation and intranasally inoculated with 50-µL virus diluted in phosphate-buffered saline (PBS). Control mice were inoculated with 50-µL PBS.

Lung virus titers

Mice were humanely euthanized; lungs were collected at set time points, homogenized in 1-mL cold PBS, and centrifuged; and the supernatant was aliquoted and frozen at −80°C. Individual lung homogenate aliquots were thawed and assayed for influenza virus by plaque assay on MDCK cells.

Histopathology

Mice were humanely euthanized at 2 and 4 DPI, and lungs were collected, inflated, and fixed by immersion in 10% buffered formalin. Fixed lungs were submitted to the American Association of Veterinary Laboratory Diagnosticians accredited histology laboratory in the Department of Pathology at the University of Georgia for processing

and sectioning. Briefly, lungs were embedded in paraffin so that all lung lobes could be evaluated, and 4-µm sections were cut and stained with hematoxylin and eosin. Lungs were blinded, analyzed by a diplomate of the American College of Veterinary Pathologists, and scored as follows: perivascular (bronchial tree) inflammation (0 = none, 1 = mild, 1–2 cells wide; 2 = moderate, 3–10 cells wide; 3 = severe, >10 cells wide); percentage of bronchioles affected (0 = none; 1 ≤ 25%, 2 = 25%–75%, 3 ≥ 75%); peribronchiolar inflammation (0 = none, 1 = mild, 2 = moderate, and 3 = severe); severity of airway luminal exudate, epithelial necrosis and inflammation (0 = none, 1 = mild, 2 = moderate, and 3 = severe); percentage of alveolar involvement (0 = none, 1 ≤ 25%, 2 = 25%–50%, 3 ≥ 50%); severity of interstitial inflammation (0 = none, 1 = mild, 2 = moderate, and 3 = severe); edema (0 = none and 1 = present); hemorrhage (0 = none and 1 = present); type II cell hyperplasia (0 = none and 1 = present); and vasculitis (0 = none and 1 = present). This resulted in scores ranging from 0 to 22. BALT (well defined aggregates of mixed lymphocytes or follicles) was scored separately as 0–3 (0 = none, 1 = mild, 2 = moderate, and 3 = severe).

Statistical analysis

Statistics were run using GraphPad Prism v.7.03. Statistical analysis included two-way analysis of variance with Bonferroni post hoc test for weight loss, viral titers, and lung pathology scores of H3 swFLUAVs, Dunnett post hoc test for weight loss, viral titers, and lung pathology scores of H1 swFLUAVs or Kaplan-Meier survival curve for survival data. All results were considered significant at P values of <0.05.

ACKNOWLEDGMENTS

We thank the staff of the UGA Animal Health Research Center and Animal Resources Program for their care and maintenance of the mice. We sincerely appreciate the Histology Laboratory in the Department of Pathology at the University of Georgia, specifically Dr. Elizabeth Howerth, for lung histopathological analysis. Furthermore, we are grateful to Cheryl Jones and Scott Johnson for their kind assistance in data collection. Madin-Darby Canine Kidney (MDCK-ATL) Cells, FR-926, were obtained through the International Reagent Resource, Influenza Division, WHO Collaborating Center for Surveillance, Epidemiology and Control of Influenza, Centers for Disease Control and Prevention, Atlanta, GA, USA.

This work was supported by the UGA-Emory Centers of Excellence for Influenza Research and Surveillance contract HHSN272201400004C (S.M.T.).

Conceptualization: S.J.C., C.S.K., and S.M.T.; methodology: S.J.C., L.M.F., E.F.G., and S.M.T.; formal analysis: S.J.C., L.M.F., and E.F.G.; Investigation, S.J.C., and E.F.G.; Resources, S.M.T., E.W.H., and D.R.P.; writing (original draft): S.J.C.; writing (review and editing: S.J.C., E.F.G., S.M.T., L.M.F., C.S.K., E.W.H., and D.R.P.; visualization, S.J.C., E.F.G., and S.M.T.; supervision; D.R.P. and S.M.T.; funding acquisition: S.M.T. All authors approved the manuscript for publication.

AUTHOR AFFILIATIONS

[1]Department of Infectious Diseases, University of Georgia, Athens, Georgia, USA
[2]Center for Vaccines and Immunology, University of Georgia, Athens, Georgia, USA
[3]Emory-UGA Centers of Excellence for Influenza Research and Surveillance (CEIRS), Athens, Georgia, USA
[4]Department of Population Health, Poultry Diagnostic and Research Center, College of Veterinary Medicine, University of Georgia, Athens, Georgia, USA
[5]Department of Pathology, College of Veterinary Medicine, University of Georgia, Athens, Georgia, USA

PRESENT ADDRESS

Shelly J. Curran, Critical Care Medicine Department, National Institutes of Health, Bethesda, Maryland, USA
Lucas M. Ferreri, Department of Microbiology and Immunology, Emory University School of Medicine, Atlanta, Georgia, USA
Constantinos S. Kyriakis, Department of Pathobiology, Sugg Laboratory, Auburn University, Alpharetta, Georgia, USA

AUTHOR ORCIDs

Daniel R. Perez http://orcid.org/0000-0002-6569-5689
S. Mark Tompkins http://orcid.org/0000-0002-1523-5588

FUNDING

Funder	Grant(s)	Author(s)
HHS | NIH | National Institute of Allergy and Infectious Diseases (NIAID)	HHSN272201400004C	S. Mark Tompkins

AUTHOR CONTRIBUTIONS

Shelly J. Curran, Conceptualization, Formal analysis, Investigation, Methodology, Visualization, Writing – original draft, Writing – review and editing | Emily F. Griffin, Formal analysis, Investigation, Methodology, Visualization, Writing – review and editing | Lucas M. Ferreri, Formal analysis, Methodology, Writing – review and editing | Constantinos S. Kyriakis, Conceptualization, Writing – review and editing | Elizabeth W. Howerth, Formal analysis, Methodology, Writing – review and editing | Daniel R. Perez, Resources, Supervision, Writing – review and editing | S. Mark Tompkins, Conceptualization, Funding acquisition, Methodology, Resources, Supervision, Visualization, Writing – review and editing

DATA AVAILABILITY

All sequences are publicly available in GenBank. Virus isolates sequenced for this study are listed under National Center for Biotechnology Information bioproject accession number PRJNA600894.

ADDITIONAL FILES

The following material is available online.

Supplemental Material

Supplemental material (Spectrum03386-23-S0001.docx). Tables S1 and S2; Figure S1.

REFERENCES

1. Shaw ML, Palese P. 2013. Orthomyxoviridae, p 2 volumes. In Knipe DM, Howley PM (ed), Fields virology, 6th ed. Wolters Kluwer/Lippincott Williams & Wilkins Health, Philadelphia, PA.
2. Fiore AE, Bridges CB, Cox NJ. 2009. Seasonal influenza vaccines. Curr Top Microbiol Immunol 333:43–82. https://doi.org/10.1007/978-3-540-92165-3_3
3. Organization WH. 2014. Influenza (seasonal) fact sheet N211
4. Nicholson KG, Wood JM, Zambon M. 2003. Influenza. Lancet 362:1733–1745. https://doi.org/10.1016/S0140-6736(03)14854-4
5. Pinto LH, Holsinger LJ, Lamb RA. 1992. Influenza virus M2 protein has ion channel activity. Cell 69:517–528. https://doi.org/10.1016/0092-8674(92)90452-i
6. Hughey PG, Roberts PC, Holsinger LJ, Zebedee SL, Lamb RA, Compans RW. 1995. Effects of antibody to the influenza A virus M2 protein on M2 surface expression and virus assembly. Virology 212:411–421. https://doi.org/10.1006/viro.1995.1498
7. Ichinohe T, Pang IK, Iwasaki A. 2010. Influenza virus activates inflammasomes via its intracellular M2 ion channel. Nat Immunol 11:404–410. https://doi.org/10.1038/ni.1861
8. Gannagé M, Dormann D, Albrecht R, Dengjel J, Torossi T, Rämer PC, Lee M, Strowig T, Arrey F, Conenello G, Pypaert M, Andersen J, García-Sastre A, Münz C. 2009. Matrix protein 2 of influenza A virus blocks autophagosome fusion with lysosomes. Cell Host Microbe 6:367–380. https://doi.org/10.1016/j.chom.2009.09.005
9. Ren Y, Li C, Feng L, Pan W, Li L, Wang Q, Li J, Li N, Han L, Zheng X, Niu X, Sun C, Chen L. 2016. Proton channel activity of influenza A virus matrix protein 2 contributes to autophagy arrest. J Virol 90:591–598. https://doi.org/10.1128/JVI.00576-15

10. Beale R, Wise H, Stuart A, Ravenhill BJ, Digard P, Randow F. 2014. A LC3-interacting motif in the influenza A virus M2 protein is required to subvert autophagy and maintain virion stability. Cell Host Microbe 15:239–247. https://doi.org/10.1016/j.chom.2014.01.006
11. Seladi-Schulman J, Campbell PJ, Suppiah S, Steel J, Lowen AC. 2014. Filament-producing mutants of influenza A/Puerto Rico/8/1934 (H1N1) virus have higher neuraminidase activities than the spherical wild-type. PLoS One 9:e112462. https://doi.org/10.1371/journal.pone.0112462
12. Campbell PJ, Kyriakis CS, Marshall N, Suppiah S, Seladi-Schulman J, Danzy S, Lowen AC, Steel J. 2014. Residue 41 of the eurasian avian-like swine influenza a virus matrix protein modulates virion filament length and efficiency of contact transmission. J Virol 88:7569–7577. https://doi.org/10.1128/JVI.00119-14
13. Campbell PJ, Danzy S, Kyriakis CS, Deymier MJ, Lowen AC, Steel J. 2014. The M segment of the 2009 pandemic influenza virus confers increased neuraminidase activity, filamentous morphology, and efficient contact transmissibility to A/Puerto Rico/8/1934-based reassortant viruses. J Virol 88:3802–3814. https://doi.org/10.1128/JVI.03607-13
14. Olsen CW, Brown IH, Easterday BC, van Reeth K. 2006. Swine influenza a North American perspective, p 469–481. In Straw BE, Zimmerman JJ, D'Allaire S, Taylor DJ (ed), Diseases of swine, 9th ed. Blackwell Pub., Ames, Iowa.
15. Vincent AL, Lager KM, Anderson TK. 2014. A brief introduction to influenza A virus in swine. Methods Mol Biol 1161:243–258. https://doi.org/10.1007/978-1-4939-0758-8_20
16. Vincent AL, Ma W, Lager KM, Janke BH, Richt JA. 2008. Swine influenza viruses a North American perspective. Adv Virus Res 72:127–154. https://doi.org/10.1016/S0065-3527(08)00403-X
17. Olsen CW. 2002. The emergence of novel swine influenza viruses in North America. Virus Res 85:199–210. https://doi.org/10.1016/s0168-1702(02)00027-8
18. Zhou NN, Senne DA, Landgraf JS, Swenson SL, Erickson G, Rossow K, Liu L, Yoon K j, Krauss S, Webster RG. 1999. Genetic reassortment of avian, swine, and human influenza A viruses in American pigs. J Virol 73:8851–8856. https://doi.org/10.1128/JVI.73.10.8851-8856.1999
19. Evseenko VA, Boon ACM, Brockwell-Staats C, Franks J, Rubrum A, Daniels CS, Gramer MR, Webby RJ. 2011. Genetic composition of contemporary swine influenza viruses in the West central region of the United States of America. Influenza Other Respir Viruses 5:188–197. https://doi.org/10.1111/j.1750-2659.2010.00189.x
20. Nfon CK, Berhane Y, Hisanaga T, Zhang S, Handel K, Kehler H, Labrecque O, Lewis NS, Vincent AL, Copps J, Alexandersen S, Pasick J. 2011. Characterization of H1N1 swine influenza viruses circulating in Canadian pigs in 2009. J Virol 85:8667–8679. https://doi.org/10.1128/JVI.00801-11
21. Nfon C, Berhane Y, Zhang S, Handel K, Labrecque O, Pasick J. 2011. Molecular and antigenic characterization of triple-reassortant H3N2 swine influenza viruses isolated from pigs, Turkey and quail in Canada. Transbound Emerg Dis 58:394–401. https://doi.org/10.1111/j.1865-1682.2011.01219.x
22. Lorusso A, Vincent AL, Harland ML, Alt D, Bayles DO, Swenson SL, Gramer MR, Russell CA, Smith DJ, Lager KM, Lewis NS. 2011. Genetic and antigenic characterization of H1 influenza viruses from United States swine from 2008. J Gen Virol 92:919–930. https://doi.org/10.1099/vir.0.027557-0
23. Novel Swine-Origin Influenza A, Dawood FS, Jain S, Finelli L, Shaw MW, Lindstrom S, Garten RJ, Gubareva LV, Xu X, Bridges CB, Uyeki TM. 2009. Emergence of a novel swine-origin influenza A (H1N1) virus in humans. N Engl J Med 360:2605–2615. https://doi.org/10.1056/NEJMoa0903810
24. Watson SJ, Langat P, Reid SM, Lam TT-Y, Cotten M, Kelly M, Van Reeth K, Qiu Y, Simon G, Bonin E, et al. 2015. Molecular epidemiology and evolution of influenza viruses circulating within European swine between 2009 and 2013. J Virol 89:9920–9931. https://doi.org/10.1128/JVI.00840-15
25. Simon G, Larsen LE, Dürrwald R, Foni E, Harder T, Van Reeth K, Markowska-Daniel I, Reid SM, Dan A, Maldonado J, Huovilainen A, Billinis C, Davidson I, Agüero M, Vila T, Hervé S, Breum SØ, Chiapponi C, Urbaniak K, Kyriakis CS, Brown IH, Loeffen W, ESNIP3 consortium. 2014. European surveillance network for influenza in pigs: surveillance programs, diagnostic tools and swine influenza virus subtypes. PLoS One 9:e115815. https://doi.org/10.1371/journal.pone.0115815
26. Nelson MI, Viboud C, Vincent AL, Culhane MR, Detmer SE, Wentworth DE, Rambaut A, Suchard MA, Holmes EC, Lemey P. 2015. Global migration of influenza A viruses in swine. Nat Commun 6:6696. https://doi.org/10.1038/ncomms7696
27. Nelson MI, Stratton J, Killian ML, Janas-Martindale A, Vincent AL. 2015. Continual reintroduction of human pandemic H1N1 influenza A viruses into swine in the United States. J Virol 89:6218–6226. https://doi.org/10.1128/JVI.00459-15
28. Kyriakis CS, Zhang M, Wolf S, Jones LP, Shim BS, Chocallo AH, Hanson JM, Jia M, Liu D, Tripp RA. 2017. Molecular epidemiology of swine influenza A viruses in the southeastern United States, highlights regional differences in circulating strains. Vet Microbiol 211:174–179. https://doi.org/10.1016/j.vetmic.2017.10.016
29. Takemae N, Harada M, Nguyen PT, Nguyen T, Nguyen TN, To TL, Nguyen TD, Pham VP, Le VT, Do HT, Vo HV, Le QVT, Tran TM, Nguyen TD, Thai PD, Nguyen DH, Le AQT, Nguyen DT, Uchida Y, Saito T. 2017. Influenza A viruses of swine (IAV-S) in Vietnam from 2010 to 2015: multiple introductions of A(H1N1)pdm09 viruses into the pig population and diversifying genetic constellations of enzootic IAV-S. J Virol 91:e01490-16. https://doi.org/10.1128/JVI.01490-16
30. Rajão DS, Walia RR, Campbell B, Gauger PC, Janas-Martindale A, Killian ML, Vincent AL. 2017. Reassortment between swine H3N2 and 2009 pandemic H1N1 in the United States resulted in influenza A viruses with diverse genetic constellations with variable virulence in pigs. J Virol 91:e01763-16. https://doi.org/10.1128/JVI.01763-16
31. Song Y, Wu X, Wang N, Ouyang G, Qu N, Cui J, Qi Y, Liao M, Jiao P. 2016. A novel H1N2 influenza virus related to the classical and human influenza viruses from pigs in Southern China. Front Microbiol 7:1068. https://doi.org/10.3389/fmicb.2016.01068
32. Mukherjee A, Nayak MK, Dutta S, Panda S, Satpathi BR, Chawla-Sarkar M, Manicassamy B. 2016. Genetic characterization of circulating 2015 A(H1N1)pdm09 influenza viruses from Eastern India. PLoS ONE 11:e0168464. https://doi.org/10.1371/journal.pone.0168464
33. Walia RR, Anderson TK, Vincent AL. 2019. Regional patterns of genetic diversity in swine influenza A viruses in the United States from 2010 to 2016. Influenza Other Respir Viruses 13:262–273. https://doi.org/10.1111/irv.12559
34. Anderson TK, Nelson MI, Kitikoon P, Swenson SL, Korslund JA, Vincent AL. 2013. Population dynamics of cocirculating swine influenza A viruses in the United States from 2009 to 2012. Influenza Other Respir Viruses 7 Suppl 4:42–51. https://doi.org/10.1111/irv.12193
35. Kitikoon P, Nelson MI, Killian ML, Anderson TK, Koster L, Culhane MR, Vincent AL. 2013. Genotype patterns of contemporary reassorted H3N2 virus in US swine. J Gen Virol 94:1236–1241. https://doi.org/10.1099/vir.0.51839-0
36. Bowman AS, Nolting JM, Nelson SW, Slemons RD. 2012. Subclinical influenza virus A infections in pigs exhibited at agricultural fairs. Emerg Infect Dis 18:1945–1950. https://doi.org/10.3201/eid1812.121116
37. Calderon BM, Danzy S, Delima GK, Jacobs NT, Ganti K, Hockman MR, Conn GL, Lowen AC, Steel J. 2019. Dysregulation of M segment gene expression contributes to influenza A virus host restriction. PLoS Pathog 15:e1007892. https://doi.org/10.1371/journal.ppat.1007892
38. Furuse Y, Suzuki A, Kamigaki T, Oshitani H. 2009. Evolution of the M gene of the influenza A virus in different host species: large-scale sequence analysis. Virol J 6:67. https://doi.org/10.1186/1743-422X-6-67
39. Lakdawala SS, Lamirande EW, Suguitan AL, Wang W, Santos CP, Vogel L, Matsuoka Y, Lindsley WG, Jin H, Subbarao K. 2011. Eurasian-origin gene segments contribute to the transmissibility, aerosol release, and morphology of the 2009 pandemic H1N1 influenza virus. PLoS Pathog 7:e1002443. https://doi.org/10.1371/journal.ppat.1002443
40. Samet SJ, Tompkins SM. 2017. Influenza pathogenesis in genetically defined resistant and susceptible murine strains. Yale J Biol Med 90:471–479.
41. Pica N, Iyer A, Ramos I, Bouvier NM, Fernandez-Sesma A, García-Sastre A, Lowen AC, Palese P, Steel J. 2011. The DBA.2 mouse is susceptible to disease following infection with a broad, but limited, range of influenza A and B viruses. J Virol 85:12825–12829. https://doi.org/10.1128/JVI.05930-11
42. Kim JI, Park S, Lee S, Lee I, Heo J, Hwang MW, Bae JY, Kim D, Jang SI, Park MS, Park MS. 2013. DBA/2 mouse as an animal model for anti-influenza

drug efficacy evaluation. J Microbiol 51:866–871. https://doi.org/10.1007/s12275-013-3428-7
43. Margine I, Krammer F. 2014. Animal models for influenza viruses: implications for universal vaccine development. Pathogens 3:845–874. https://doi.org/10.3390/pathogens3040845
44. Boon ACM, Finkelstein D, Zheng M, Liao G, Allard J, Klumpp K, Webster R, Peltz G, Webby RJ. 2011. H5N1 influenza virus pathogenesis in genetically diverse mice is mediated at the level of viral load. mBio 2:1–10. https://doi.org/10.1128/mBio.00171-11
45. Bouvier NM, Lowen AC. 2010. Animal models for influenza virus pathogenesis and transmission. Viruses 2:1530–1563. https://doi.org/10.3390/v20801530
46. Boon ACM, deBeauchamp J, Hollmann A, Luke J, Kotb M, Rowe S, Finkelstein D, Neale G, Lu L, Williams RW, Webby RJ. 2009. Host genetic variation affects resistance to infection with a highly pathogenic H5N1 influenza A virus in mice. J Virol 83:10417–10426. https://doi.org/10.1128/JVI.00514-09
47. Srivastava B, Błazejewska P, Hessmann M, Bruder D, Geffers R, Mauel S, Gruber AD, Schughart K. 2009. Host genetic background strongly influences the response to influenza a virus infections. PLoS One 4:e4857. https://doi.org/10.1371/journal.pone.0004857
48. Trammell RA, Liberati TA, Toth LA. 2012. Host genetic background and the innate inflammatory response of lung to influenza virus. Microbes Infect 14:50–58. https://doi.org/10.1016/j.micinf.2011.08.008
49. Casanova T, Van de Paar E, Desmecht D, Garigliany M-M. 2015. Hyporeactivity of alveolar Macrophages and higher respiratory cell Permissivity characterize DBA/2J mice infected by influenza A virus. J Interferon Cytokine Res 35:808–820. https://doi.org/10.1089/jir.2014.0237
50. Bogdanow B, Wang X, Eichelbaum K, Sadewasser A, Husic I, Paki K, Budt M, Hergeselle M, Vetter B, Hou J, Chen W, Wiebusch L, Meyer IM, Wolff T, Selbach M. 2019. The dynamic proteome of influenza A virus infection identifies M segment splicing as a host range determinant. Nat Commun 10:5518. https://doi.org/10.1038/s41467-019-13520-8
51. Almansa R, Martínez-Orellana P, Rico L, Iglesias V, Ortega A, Vidaña B, Martínez J, Expósito A, Montoya M, Bermejo-Martin JF. 2017. Pulmonary transcriptomic responses indicate a dual role of inflammation in pneumonia development and viral clearance during 2009 pandemic influenza infection. PeerJ 5:e3915. https://doi.org/10.7717/peerj.3915
52. Cao W, Mishina M, Ranjan P, De La Cruz JA, Kim JH, Garten R, Kumar A, García-Sastre A, Katz JM, Gangappa S, Sambhara S. 2015. A newly emerged swine-origin influenza A(H3N2) variant dampens host antiviral immunity but induces potent inflammasome activation. J Infect Dis 212:1923–1929. https://doi.org/10.1093/infdis/jiv330
53. Taubenberger JK, Morens DM. 2008. The pathology of influenza virus infections. Annu Rev Pathol 3:499–522. https://doi.org/10.1146/annurev.pathmechdis.3.121806.154316
54. de Jong MD, Simmons CP, Thanh TT, Hien VM, Smith GJD, Chau TNB, Hoang DM, Chau NVV, Khanh TH, Dong VC, Qui PT, Cam BV, Ha DQ, Guan Y, Peiris JSM, Chinh NT, Hien TT, Farrar J. 2006. Fatal outcome of human influenza A (H5N1) is associated with high viral load and hypercytokinemia. Nat Med 12:1203–1207. https://doi.org/10.1038/nm1477
55. Perrone LA, Plowden JK, García-Sastre A, Katz JM, Tumpey TM. 2008. H5N1 and 1918 pandemic influenza virus infection results in early and excessive infiltration of macrophages and neutrophils in the lungs of mice. PLoS Pathog 4:e1000115. https://doi.org/10.1371/journal.ppat.1000115
56. Szretter KJ, Gangappa S, Lu X, Smith C, Shieh W-J, Zaki SR, Sambhara S, Tumpey TM, Katz JM. 2007. Role of host cytokine responses in the pathogenesis of avian H5N1 influenza viruses in mice. J Virol 81:2736–2744. https://doi.org/10.1128/JVI.02336-06
57. Tumpey TM, García-Sastre A, Taubenberger JK, Palese P, Swayne DE, Pantin-Jackwood MJ, Schultz-Cherry S, Solórzano A, Van Rooijen N, Katz JM, Basler CF. 2005. Pathogenicity of influenza viruses with genes from the 1918 pandemic virus: functional roles of alveolar macrophages and neutrophils in limiting virus replication and mortality in mice. J Virol 79:14933–14944. https://doi.org/10.1128/JVI.79.23.14933-14944.2005
58. Park HS, Liu G, Thulasi Raman SN, Landreth SL, Liu Q, Zhou Y. 2018. NS1 protein of 2009 pandemic influenza A virus inhibits porcine NLRP3 inflammasome-mediated interleukin-1 beta production by suppressing ASC ubiquitination. J Virol 92:e00022-18. https://doi.org/10.1128/JVI.00022-18
59. Metreveli G, Gao Q, Mena I, Schmolke M, Berg M, Albrecht RA, García-Sastre A. 2014. The origin of the PB1 segment of swine influenza A virus subtype H1N2 determines viral pathogenicity in mice. Virus Res 188:97–102. https://doi.org/10.1016/j.virusres.2014.03.023
60. Zhu J, Jiang Z, Liu J. 2021. The matrix gene of pdm/09 H1N1 contributes to the pathogenicity and transmissibility of SIV in mammals. Vet Microbiol 255:109039. https://doi.org/10.1016/j.vetmic.2021.109039
61. Bialas KM, Bussey KA, Stone RL, Takimoto T. 2014. Specific nucleoprotein residues affect influenza virus morphology. J Virol 88:2227–2234. https://doi.org/10.1128/JVI.03354-13
62. Biswas SK, Boutz PL, Nayak DP. 1998. Influenza virus nucleoprotein interacts with influenza virus polymerase proteins. J Virol 72:5493–5501. https://doi.org/10.1128/JVI.72.7.5493-5501.1998
63. Davis AM, Ramirez J, Newcomb LL. 2017. Identification of influenza A nucleoprotein body domain residues essential for viral RNA expression expose antiviral target. Virol J 14:22. https://doi.org/10.1186/s12985-017-0694-8
64. Gao Q, Chou YY, Doğanay S, Vafabakhsh R, Ha T, Palese P. 2012. The influenza A virus PB2, PA, NP, and M segments play a pivotal role during genome packaging. J Virol 86:7043–7051. https://doi.org/10.1128/JVI.00662-12
65. Nguyen NLT, Wu W, Panté N. 2023. Contribution of the nuclear localization sequences of influenza A nucleoprotein to the nuclear import of the influenza genome in infected cells. Viruses 15:1641. https://doi.org/10.3390/v15081641
66. Zhu W, Feng Z, Chen Y, Yang L, Liu J, Li X, Liu S, Zhou L, Wei H, Gao R, Wang D, Shu Y. 2019. Mammalian-adaptive mutation NP-Q357K in eurasian H1N1 swine influenza viruses determines the virulence phenotype in mice. Emerg Microbes Infect 8:989–999. https://doi.org/10.1080/22221751.2019.1635873
67. Bakre AA, Jones LP, Kyriakis CS, Hanson JM, Bobbitt DE, Bennett HK, Todd KV, Orr-Burks N, Murray J, Zhang M, Steinhauer DA, Byrd-Leotis L, Cummings RD, Fent J, Coffey T, Tripp RA. 2020. Molecular epidemiology and glycomics of swine influenza viruses circulating in commercial swine farms in the Southeastern and Midwest United States. Vet Microbiol 251:108914. https://doi.org/10.1016/j.vetmic.2020.108914
68. Mooney AJ, Gabbard JD, Li Z, Dlugolenski DA, Johnson SK, Tripp RA, He B, Tompkins SM. 2017. Vaccination with recombinant parainfluenza virus 5 expressing neuraminidase protects against homologous and heterologous influenza virus challenge. J Virol 91:e01579-17. https://doi.org/10.1128/JVI.01579-17
69. Mena I, Nelson MI, Quezada-Monroy F, Dutta J, Cortes-Fernández R, Lara-Puente JH, Castro-Peralta F, Cunha LF, Trovão NS, Lozano-Dubernard B, Rambaut A, van Bakel H, García-Sastre A. 2016. Origins of the 2009 H1N1 influenza pandemic in swine in Mexico. eLife 5:e16777. https://doi.org/10.7554/eLife.16777
70. Grabherr MG, Haas BJ, Yassour M, Levin JZ, Thompson DA, Amit I, Adiconis X, Fan L, Raychowdhury R, Zeng Q, Chen Z, Mauceli E, Hacohen N, Gnirke A, Rhind N, di Palma F, Birren BW, Nusbaum C, Lindblad-Toh K, Friedman N, Regev A. 2011. Full-length transcriptome assembly from RNA-seq data without a reference genome. Nat Biotechnol 29:644–652. https://doi.org/10.1038/nbt.1883
71. Kent WJ. 2002. BLAT--the BLAST-like alignment tool. Genome Res 12:656–664. https://doi.org/10.1101/gr.229202
72. Li H, Durbin R. 2009. Fast and accurate short read alignment with burrows-wheeler transform. Bioinform 25:1754–1760. https://doi.org/10.1093/bioinformatics/btp324